



Contents lists available at ScienceDirect

Automatica

journal homepage: www.elsevier.com/locate/automatica

Brief paper

Generalization of the twisting convergence conditions to non-affine systems[☆]

Dominique Monnet^{a,*}, Alexandre Goldsztejn^b, Franck Plestan^a

^a École Centrale de Nantes-LS2N, UMR CNRS 6004, 1 rue de la Noë, 44300 Nantes, France

^b Centre National de la Recherche Scientifique-LS2N, UMR CNRS 6004, 1 rue de la Noë, 44300 Nantes, France

ARTICLE INFO

Article history:

Received 28 September 2020

Received in revised form 28 February 2021

Accepted 21 September 2021

Available online xxxx

Keywords:

Twisting control

Nonlinear system

Non-affine system

ABSTRACT

The twisting algorithm is a second order sliding mode technique for which convergence conditions have been established. However, these conditions are limited to systems that are affine in the control. In this paper, new convergence conditions that are not limited to such systems, are proposed. Furthermore, it is shown that in the affine case, state-of-the-art convergence conditions are more conservative than the new conditions. Two examples illustrate the difference of conservatism and the way that the new conditions ensure the convergence of systems non-affine in the control input.

© 2021 Published by Elsevier Ltd.

1. Introduction

Sliding-mode control is now a well-established control theory (Edwards & Spurgeon, 1998; Shtessel, Edwards, Fridman, & Levant, 2014; Utkin, 2013). The principle is to drive and maintain the system trajectory on a manifold, called “sliding surface” with a discontinuous control signal, in spite of perturbations and uncertainties. While evolving on this surface, the system has the desired dynamic, and is not sensitive to these perturbations and uncertainties.

An undesirable effect of the discontinuous control signal is the so-called chattering effect (Boiko, 2005; Fridman, 2003; Levant, 2010), that is a high-frequency oscillations phenomenon that can damage actuators. In order to attenuate the chattering, higher order sliding mode techniques have been developed, in contrast with the standard first order sliding mode. Among the higher order sliding mode techniques (see for example Fridman, Barbot, & Plestan, 2016; Shtessel et al., 2014), second order sliding-mode (2-SM) control has been extensively studied and successfully applied to real case problems. Recent works propose advanced 2-SM methods based on discontinuous sliding surfaces depending

on quantization levels of the uncertainties to further limit control amplitude (Ferrara, Incremona, & Cucuzzella, 2019; Incremona, Cucuzzella, & Ferrara, 2017) and chattering.

2-SM can be achieved through different controller structures. The approach based on the contractivity property of differential inclusion has provided 2-SM establishment conditions for several 2-SM controllers (Levant, 1993, 1998, 2007) (among them, the twisting algorithm and the super-twisting controllers). Lyapunov-based conditions for 2-SM establishment have been proposed for twisting (Polyakov & Poznyak, 2009; Utkin, Guldner, & Jingxin, 2009) or super-twisting (Moreno & Osorio, 2008, 2012) controllers, and for their adaptive extensions (Shtessel, Moreno, & Fridman, 2017; Shtessel, Moreno, Plestan, Fridman, & Poznyak, 2010; Shtessel, Taleb, & Plestan, 2012). These convergence conditions, derived either from the contractivity property or from Lyapunov theory, are sufficient but not necessary. Weaker convergence conditions are of great benefit: they allow more freedom in choosing controller parameters when designing a controller, generally leading to improved designs.

In this paper, we focus on the twisting trajectories typically obtained using a twisting controller. By investigating the finite time convergence of these twisting trajectories independently of any controller structure, we obtain new finite time convergence conditions that apply to systems with non-affine control input and no assumption on the controller structure. In addition to the novelty of handling non-affine control inputs and non-twisting controller structures, these new sufficient conditions turn out to be sensibly weaker than the previously proposed conditions (Levant, 2007; Polyakov & Poznyak, 2009; Utkin et al., 2009) when restricted to affine input systems with twisting controller.

This paper is organized as follows. Section 2 explains the proposed approach to generalizing convergence conditions to

[☆] This work was partially supported by Région Pays de la Loire, Centrale Nantes, West Atlantic Marine Energy Community, LS2N and CNRS as part of the O2GRACE project. This work was partially supported by the French Agence Nationale de la Recherche (ANR) Grant Number ANR-16-CE33-0024. The material in this paper was not presented at any conference. This paper was recommended for publication in revised form by Associate Editor Luca Zaccarian under the direction of Editor Daniel Liberzon.

* Corresponding author.

E-mail addresses: dominique.monnet@ec-nantes.fr (D. Monnet), alexandre.goldsztejn@ec-nantes.fr (A. Goldsztejn), franck.plestan@ec-nantes.fr (F. Plestan).

Table 1

Summary on bound definitions and convergence conditions presented in the paper, from the more conservative to the less conservative. [Corollaries 1.2](#) and [1.1](#) are restricted to affine control inputs and to the twisting controller, i.e., $\ddot{\sigma} = h(t, x) + g(t, x)(-r_1 \text{sign}(\sigma) - r_2 \text{sign}(\dot{\sigma}))$. On the contrary, [Theorem 1](#) makes no hypothesis on the system or the controller, therefore the design parameters of the controller do not appear explicitly in the constraints.

	Bounds to be computed	Sufficient condition for finite time convergence
Levant (Shtessel et al., 2014 , pp. 148) (Corollary 1.2)	C, k, K s.t. $h(t, x) \in [-C, C], g(t, x) \in [k, K],$ $\forall t \geq 0, \forall x \in X$	$0 < k, 0 < r_2 < r_1$ $C < k(r_1 - r_2)$ $(r_1 - r_2)K + C < (r_1 + r_2)k - C$
Corollary 1.1	$c_i, C_i, k_i, K_i, i \in \{1, \dots, 4\}$ s.t. $h(t, x) \in [c_i, C_i], g(t, x) \in [k_i, K_i],$ $\forall t \geq 0, \forall x \in X_i(t)$	$0 < k_i, 0 < r_2 < r_1$ $C_1 < k_1(r_1 + r_2), C_2 < k_2(r_1 - r_2)$ $-c_3 < k_3(r_1 + r_2), -c_4 < k_4(r_1 - r_2)$ $(C_1 + k_1(-r_1 - r_2))(c_3 + k_3(r_1 + r_2))$ $< (c_2 + K_2(-r_1 + r_2))(C_4 + K_4(r_1 - r_2))$
Theorem 1	$m_i, M_i, i \in \{1, \dots, 4\}$ s.t. $\ddot{\sigma}(t, x) \in [m_i, M_i]$ $\forall t \geq 0, \forall x \in X_i(t)$	$M_1 < 0, M_2 < 0, 0 < m_3, 0 < m_4$ $M_1 m_3 < m_2 M_4$

non-affine systems. Section 3 provides a theorem that states the convergence conditions of the twisting trajectory. This theorem leads to two corollaries that give sufficient conditions on the twisting controller's parameters to ensure finite time 2-SM establishment. Through two academic examples, Section 4 illustrates that the new convergence conditions are less conservative than the state-of-the-art ones and can be applied to non-affine systems. Finally, Section 5 summarizes the results and provides directions for future works.

2. Proposed approach

Consider single input non-linear system given by the differential equation,

$$\dot{x} = f(t, x, u), \quad (1)$$

where $x \in \mathbb{R}^n$ is the state vector and $u \in \mathbb{R}$ is the control input. The sliding variable is denoted $\sigma(t, x)$, and it is supposed that the system has a relative degree of 2, i.e., $\dot{\sigma}$ does not depend on u while u explicitly appears in the expression of $\ddot{\sigma}$,

$$\ddot{\sigma} = \ddot{\sigma}(t, x, u). \quad (2)$$

The function $\sigma(t, x)$ is differentiable, $\dot{\sigma}(t, x)$ is continuous and $\ddot{\sigma}(t, x, u)$ is typically discontinuous because u is discontinuous. The control objective consists in forcing σ to zero, and we assume that u is a function of σ and $\dot{\sigma}$,

$$u = \varphi(\sigma, \dot{\sigma}). \quad (3)$$

In the context of 2-SM, φ is discontinuous. We assume that a trajectory $x(t)$ exists $\forall t \geq 0$ in the sense of Filippov ([Filippov, 2010](#)), and that $x(t) \in X \subseteq \mathbb{R}^n$, with X a compact.

Usually, the time dependency of $\sigma(t)$, $\dot{\sigma}(t)$ and $\ddot{\sigma}(t)$ refers to some dependency to perturbations $p(t)$. In that case, we assume known bounds $p(t) \in [p_{min}, p_{max}]$ that hold $\forall t \geq 0$.

2.1. The twisting controller

In the particular case where f is affine in u , the second time derivative of the sliding variable is also affine in u , that is, (2) becomes,

$$\ddot{\sigma} = h(t, x) + g(t, x)u(t). \quad (4)$$

Consider the following well-known twisting controller ([Levant, 1993](#))

$$\varphi(\sigma, \dot{\sigma}) = -r_1 \text{sign}(\sigma) - r_2 \text{sign}(\dot{\sigma}), \quad (5)$$

where $r_1 > r_2 > 0$. In [Shtessel et al. \(2014, pp. 148\)](#), the principle of the finite-time convergence proof relies on the following global bounds on $h(t, x)$ and $g(t, x)$,

$$h(t, x) \in [-C, C], g(t, x) \in [k, K], \forall x \in X, \forall t \geq 0, \quad (6)$$

with $k > 0$, which further ensures $g(t, x) > 0$. Those bounds allow enclosing the dynamic of $\sigma(t)$ in the following differential inclusion in the phase plan $(\sigma, \dot{\sigma})$:

$$\dot{\sigma} \in [-C, C] + [k, K]\varphi(\sigma, \dot{\sigma}). \quad (7)$$

This problem being two-dimensional, a majorant curve in the phase plan $(\sigma, \dot{\sigma})$ can be used to capture all possible trajectories, and the finite-time convergence of this majorant curve to the origin holds true for all the possible trajectories. The resulting sufficient convergence conditions depending on the parameter r_1 and r_2 are given in the first line of [Table 1](#).

2.2. Generalized twisting conditions

The finite time convergence of the trajectories generated by the twisting controller is the consequence of behavior of the differential inclusion (7) that differs in each of the four orthants Σ_i

$$\begin{aligned} \Sigma_1 &= \{(\sigma, \dot{\sigma}) \mid \sigma > 0 \text{ and } \dot{\sigma} > 0\}, \\ \Sigma_2 &= \{(\sigma, \dot{\sigma}) \mid \sigma > 0 \text{ and } \dot{\sigma} < 0\}, \\ \Sigma_3 &= \{(\sigma, \dot{\sigma}) \mid \sigma < 0 \text{ and } \dot{\sigma} < 0\}, \\ \Sigma_4 &= \{(\sigma, \dot{\sigma}) \mid \sigma < 0 \text{ and } \dot{\sigma} > 0\}. \end{aligned} \quad (8)$$

While in the standard approach the orthant dependent dynamic enforced by the twisting controller is analyzed, we propose here another approach: We directly analyze the conditions on the orthant dependent dynamic to produce a finite time convergence, independently of the system structure (that may be non-affine in the input) and of the controller structure. Such conditions naturally involve bounds m_i and M_i on the dynamic that are defined orthant-wise:

$$\ddot{\sigma} \in [m_i, M_i], \forall (\sigma, \dot{\sigma}) \in \Sigma_i, \quad (9)$$

which are foreseen to be less conservative than the bounds (6) since the latter hold in all orthants. In practice, orthant dependent bounds are evaluated on each

$$X_i(t) = \{x \in X \mid (\sigma(t, x), \dot{\sigma}(t, x)) \in \Sigma_i\} \quad (10)$$

instead of being evaluated on the whole space X :

$$\ddot{\sigma}(t, x) \in [m_i, M_i], \forall t \geq 0, \forall x \in X_i(t). \quad (11)$$

Computing such bounds in each of the four orthants roughly requires four times more work, but this is advisable in a design phase aiming to obtain a less conservative design. Those general sufficient conditions are stated in [Theorem 1](#) and summarized in the last line of [Table 1](#). In [Table 1](#) and in the rest of the paper, bounds that need to hold $\forall t \geq 0$ are usually enforced to hold $\forall p \in [p_{min}, p_{max}]$.

This general approach is finally instantiated to systems with an affine input and the twisting controller. The resulting sufficient

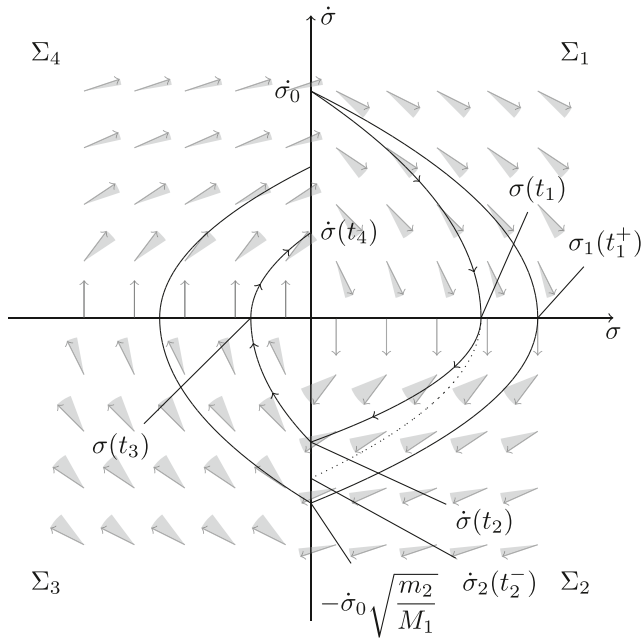


Fig. 1. Illustration of [Theorem 1](#). The arrowed curve represents a possible trajectory and the solid curve the majorant curve. The dotted curve bounds any trajectory from the initial condition $(\sigma(t_1), 0)$. The cones represent the set vector field obtained with the differential inclusion (9), and the black arrows the vector field that provides the majorant curve.

conditions are stated in [Corollary 1.1](#). They are summarized in the second line of [Table 1](#): A comparison with the first line of the table shows that they are similar to the usual sufficient conditions associated to the twisting controller, but defined orthant-wise and are therefore less conservative.

3. Conditions of convergence

3.1. General case

Consider differential inclusion (9). Sufficient conditions on the bounds m_i, M_i are given in the next theorem ([Theorem 1](#)), to ensure the finite-time convergence of σ and $\dot{\sigma}$ to zero in finite time with a twisting trajectory.

First, in the half plan $\sigma \geq 0$, having $\ddot{\sigma} < 0$ ensures that the trajectory $(\sigma(t), \dot{\sigma}(t))$ crosses the semi-axis $\dot{\sigma} \leq 0$ in finite time in the phase diagram, and vice-versa in the half plan $\sigma \leq 0$. This corresponds to Conditions (13) and (14) of [Theorem 1](#).

Secondly, every time the trajectory crosses the same semi-axis, it must get closer to the origin. It is shown in the proof that the ratio between the two consecutive intersection points along the same semi-axis is bounded by

$$\frac{|m_2 M_4|}{|M_1 m_3|}, \quad (12)$$

and having this ratio strictly lower than one, corresponding to Condition (15), ensures the finite-time convergence to the origin.

Theorem 1. *If differential inclusion (9) holds,*

$$M_1, M_2 < 0, \quad (13)$$

$$m_3, m_4 > 0, \quad (14)$$

and

$$\frac{|m_2 M_4|}{|M_1 m_3|} < 1, \quad (15)$$

then σ and $\dot{\sigma}$ converge to zero in finite time. Moreover, with the initial conditions $\sigma_0 = 0$ and $\dot{\sigma}_0 > 0$, the convergence time is lower than

$$d \frac{\dot{\sigma}_0}{1-q}, \quad (16)$$

where d and $q < 1$ are defined by,

$$d = -\frac{1}{M_1} + \frac{1}{\sqrt{M_1 M_2}} + \frac{1}{m_3} \sqrt{\frac{m_2}{M_1}} + \sqrt{\frac{m_2}{M_1 m_3 m_4}} \quad (17)$$

$$q = \sqrt{\frac{m_2 M_4}{M_1 m_3}}. \quad \blacksquare$$

Proof. Consider the initial condition $\sigma = 0, \dot{\sigma} = \dot{\sigma}_0 > 0$ at time $t = 0$. Due to Condition (13), $\dot{\sigma}$ is strictly decreasing over time and reaches 0 in a finite time denoted $t_1, \dot{\sigma}(t_1) = 0$. In the sub-space Σ_1 , since $\ddot{\sigma}$ is upper bounded by M_1 , the trajectory $(\sigma(t), \dot{\sigma}(t))$ is externally bounded by the trajectory obtained by integrating M_1 , which is the so-called majorant curve ([Shtessel et al., 2014, ch.4](#)), [Davila, Fridman, and Levant \(2005\)](#)), as represented in [Fig. 1](#). Integrating the upper bound M_1 provides the trajectory $(\sigma_1(t), \dot{\sigma}_1(t))$, with,

$$\dot{\sigma}_1(t) = M_1 t + \dot{\sigma}_0, \quad (18)$$

$$\sigma_1(t) = \frac{1}{2} M_1 t^2 + \dot{\sigma}_0 t.$$

This bounding trajectory reaches the semi-axis $\sigma \geq 0$ at time t_1^+ ,

$$\dot{\sigma}_1(t_1^+) = 0 \iff t_1^+ = -\frac{\dot{\sigma}_0}{M_1}, \quad (19)$$

$$\sigma_1(t_1^+) = -\frac{\dot{\sigma}_0^2}{2M_1}.$$

It follows that $\sigma(t_1) \leq \sigma_1(t_1^+)$. Moreover, t_1 is upper bounded by t_1^+ . Indeed, since $\dot{\sigma} \geq 0$ and is strictly decreasing in Σ_1 ,

$$\begin{aligned} \ddot{\sigma}(t) \leq M_1 &\implies 0 \leq \dot{\sigma}(t) \leq M_1 t \\ &\implies t_1 \leq t_1^+. \end{aligned} \quad (20)$$

Consider now the sub-space Σ_2 , with the initial condition $(\sigma(t_1), 0)$. Since $\ddot{\sigma}$ is strictly negative in this sub-space, $\dot{\sigma}$ is negative strictly decreasing and the trajectory reaches the semi axis $\dot{\sigma} \leq 0$ in finite time t_2 . In this sub-space the trajectory is externally bounded by the trajectory obtained by integrating m_2 represented by the dotted curve in [Fig. 1](#). Let $t' = t - t_1$ be a fictive time variable which is such that $t = t_1 \iff t' = 0$ to simplify the following calculus. The trajectory $(\sigma_2(t'), \dot{\sigma}_2(t'))$ is given by,

$$\begin{aligned} \dot{\sigma}_2(t') &= m_2 t', \\ \sigma_2(t') &= \frac{1}{2} m_2 t'^2 + \sigma(t_1), \end{aligned} \quad (21)$$

and reaches the semi-axis $\dot{\sigma} \leq 0$ for $t' = t_2^-$,

$$\begin{aligned} \dot{\sigma}_2(t_2^-) = 0 &\iff t_2^- = \sqrt{-\frac{2\sigma(t_1)}{m_2}}, \\ \dot{\sigma}_2(t_2^-) &= -\sqrt{-2\sigma(t_1)m_2} \end{aligned} \quad (22)$$

It follows that $\dot{\sigma}(t_2) \geq \dot{\sigma}_2(t_2^-)$. Substituting $\dot{\sigma}(t_1)$ by its upper bound $\sigma_1(t_1^+)$ computed previously yields,

$$\dot{\sigma}(t_2) \geq -\dot{\sigma}_0 \sqrt{\frac{m_2}{M_1}}. \quad (23)$$

This substitution can be viewed as considering the initial condition $(\sigma_1(t_1^+), 0)$ from which integrating m_2 provides the majorant curve represented by the solid curve in Σ_2 . Let $t' = t_2^+$ be the time taken by the trajectory, obtained by integrating M_2 from $(\sigma(t_1), 0)$ at $t' = 0$, to reach the semi-axis $\dot{\sigma} \leq 0$,

$$t_2^+ = \sqrt{-\frac{2\sigma(t_1)}{M_2}}. \quad (24)$$

Since σ is positive decreasing in Σ_2 , it follows that,

$$\begin{aligned} \ddot{\sigma}(t) \leq M_2 &\iff \dot{\sigma}(t) \leq M_2 t, \\ &\iff 0 \leq \sigma(t) \leq \frac{1}{2} M_2 t^2, \end{aligned} \quad (25)$$

which implies that $\sigma(t)$ reaches zero before the trajectory obtained by integrating M_2 . This further implies that,

$$t_2 \leq t_1 + t_2^+ \iff t_2 - t_1 \leq t_2^+. \quad (26)$$

Substituting $\sigma(t_1)$ by its upper bound $\sigma_1(t_1^+)$ in the expression of t_2^+ yields the upper bound,

$$t_2^+ \leq \frac{\dot{\sigma}_0}{\sqrt{M_1 M_2}}. \quad (27)$$

Following the same reasoning as previously in the half plan $\sigma \leq 0$ for $t \geq t_2$, with t_3 and t_4 the times when the trajectory reaches the semi-axis $\sigma \leq 0$ and $\dot{\sigma} \geq 0$, respectively, we obtain,

$$t_3 - t_2 \leq t_3^+, \quad \sigma(t_3) \leq \sigma_3^+, \quad t_4 - t_3 \leq t_4^+, \quad \dot{\sigma}(t_4) \leq \dot{\sigma}_4^+. \quad (28)$$

The majorant curve is given by integrating m_3 in Σ_3 and Σ_4 in Σ_4 , and the bounds are expressed as

$$t_3^+ = -\frac{\dot{\sigma}(t_2)}{m_3}, \quad (29)$$

$$\sigma_3^- = -\frac{\dot{\sigma}(t_2)^2}{2m_3}, \quad (30)$$

$$t_4^+ = \sqrt{-2\frac{\sigma(t_3)}{m_4}}, \quad (31)$$

$$\dot{\sigma}_4^+ = \sqrt{-2\sigma(t_3)M_4}. \quad (32)$$

Substituting $\dot{\sigma}(t_2)$ by its lower bound and t_2 by its upper bounds in (29) and (30) yields,

$$t_3^+ \leq \frac{\dot{\sigma}_0}{m_3} \sqrt{\frac{m_2}{M_1}}, \quad (33)$$

$$-\frac{\dot{\sigma}_0^2 m_2}{2M_1 m_3} \leq \sigma_3^- \quad (34)$$

Substituting σ_3^- by (34) in (31) and (32) finally yields,

$$\dot{\sigma}(t_4) \leq \dot{\sigma}_0 \sqrt{\frac{m_2 M_4}{M_1 m_3}}, \quad (35)$$

and

$$t_4 \leq t_1^+ + t_2^+ + t_3^+ + t_4^+ = d \dot{\sigma}_0, \quad (36)$$

where d is given by (17). Let $\dot{\sigma}_i = \dot{\sigma}(t_i)$ be the value of $\dot{\sigma}$ the i th time the trajectory crosses the semi-axis $\dot{\sigma} \geq 0$ at time t_i . From Eq. (35) and Condition (15), we have,

$$\frac{\dot{\sigma}_{i+1}}{\dot{\sigma}_i} \leq q = \sqrt{\frac{m_2 M_4}{M_1 m_3}} < 1. \quad (37)$$

As a consequence, $\dot{\sigma}(t)$ tends to zero. By Eq. (36), and since $q < 1$, the convergence time $T = \sum_{i=1}^{\infty} t_i$ is bounded by,

$$\sum_{i=1}^{\infty} t_i \leq d \sum_{i=1}^{\infty} \dot{\sigma}_{i-1} \leq d \sum_{i=1}^{\infty} q^i \dot{\sigma}_0 = d \frac{\dot{\sigma}_0}{1-q}. \quad (38)$$

This completes the proof of **Theorem 1**. ■

Theorem 1 is illustrated in **Fig. 1**. The trajectory $(\sigma(t), \dot{\sigma}(t))$ is represented by the arrowed curve, the solid curve represents majorant curve that provides the bounds on $\sigma(t_1)$, $\dot{\sigma}(t_2)$, $\sigma(t_3)$ and $\dot{\sigma}(t_4)$.

The convergence Condition (15) of **Theorem 1** does not impose that the majorant curve, and by extension any possible trajectory, have to cross the opposite semi-axes closer from the origin. For example, the ratio $\frac{m_2}{M_1}$ can be greater than one, implying that a trajectory starting from $(0, \dot{\sigma}_0)$ with $\dot{\sigma}_0 > 0$ might cross the semi-axis $\dot{\sigma} \leq 0$ at $\dot{\sigma}_1$ with $|\dot{\sigma}_1| > \dot{\sigma}_0$; the trajectory will still converge to the origin in finite time provided that Condition (15) is respected. This case is illustrated in the second example of Section 4.

Remark 1. The finite-time convergence conditions based on Lyapunov approaches generally do not allow the trajectories to get away from the origin along the axes. This is due to the fact that the proposed Lyapunov candidate functions V are symmetric with respect to the origin ($V(\sigma, \dot{\sigma}) = V(-\sigma, -\dot{\sigma})$), which implies that $V(0, \dot{\sigma}) = V(0, -\dot{\sigma})$ and $V(\sigma, 0) = V(-\sigma, 0)$ (Polyakov & Poznyak, 2009; Shtessel et al., 2017). Therefore, any trajectory starting on a semi-axis will necessarily cross the corresponding level curve of the Lyapunov candidate before crossing the opposite semi-axis further away from the origin. In that respect, any convergence conditions derived from symmetric Lyapunov functions are more conservative than the conditions of **Theorem 1**.

Theorem 1 states sufficient convergence conditions on the bounds m_i and M_i , but does not specify how these bounds are defined. So far, any bounds such that the differential inclusion (9) holds, can be used with **Theorem 1**. However, the tighter these bounds are, the greater the chances to satisfy the conditions of **Theorem 1** are.

The tightest bounds such that the differential inclusion (9) holds globally are the maxima and minima of $\ddot{\sigma}$ over Σ_i ,

$$\begin{aligned} m_i^* &= \inf_{\substack{t \geq 0 \\ x \in X_i(t)}} \ddot{\sigma}(t, x), \\ M_i^* &= \sup_{\substack{t \geq 0 \\ x \in X_i(t)}} \ddot{\sigma}(t, x). \end{aligned} \quad (39)$$

In practice, the structure of the controller is chosen to control system (1) that depends on tunable parameters, held in a vector denoted r . It follows that the bounds m_i , M_i depend on r . The problem becomes twofold: the bounds m_i , M_i , ideally the optimal ones given by (39), have to be computed and a relevant structure for the controller such that there exists r satisfying the conditions of **Theorem 1** must be chosen. In some particular cases, as illustrated in Section 4, it is possible to compute explicit expressions for the optimal bounds as functions of r and derive conditions on r from **Theorem 1**. The problem of choosing a relevant controller structure is devised in Section 4, that proposes a more general version of the twisting controller. The affine case (4) with the twisting controller (5) is easier to deal with, since it is always possible to derive explicit expressions of m_i , M_i as a function of r and to derive explicit conditions on r .

3.2. Affine case

Consider the affine case (4) with the twisting controller (5). In this case, it is possible to derive bounds on $\ddot{\sigma}$ that are expressed as linear functions of r_1 and r_2 . As a consequence, the conditions of **Theorem 1** directly provide conditions on r_1 and r_2 that enforce finite-time convergence as stated by **Corollaries 1.1** and **1.2**.

Corollary 1.1. Consider the system (4) with the twisting controller (5). Let c_i , C_i be bounds on h over the four sub-domains X_i ,

$$h(t, x) \in [c_i, C_i], \forall x \in X_i(t) \forall t \geq 0, \quad (40)$$

and k_i, K_i be bounds on g ,

$$g(t, x) \in [k_i, K_i], \forall x \in X_i(t) \forall t \geq 0. \quad (41)$$

If (r_1, r_2) satisfies

$$\begin{aligned} 0 \leq k_i, \quad i = 1, 2, 3, 4, \\ 0 < r_2 < r_1, \end{aligned} \quad (42)$$

$$\begin{aligned} C_1 < k_1(r_1 + r_2), \\ C_2 < k_2(r_1 - r_2), \end{aligned} \quad (43)$$

$$\begin{aligned} -c_3 < k_3(r_1 + r_2), \\ -c_4 < k_4(r_1 - r_2), \end{aligned} \quad (44)$$

and

$$\begin{aligned} (C_1 + k_1(-r_1 - r_2))(c_3 + k_3(r_1 + r_2)) \\ < (c_2 + K_2(-r_1 + r_2))(C_4 + K_4(r_1 - r_2)) \end{aligned} \quad (45)$$

then σ and $\dot{\sigma}$ converge to zero in finite time. ■

Proof. Condition (42) implies that $r_1 + r_2 > 0$, and the following bounds on $\ddot{\sigma}$ can be derived in Σ_1 ,

$$\begin{aligned} \ddot{\sigma}(t, x, \sigma, \dot{\sigma}) \in [c_1, C_1] - [k_1, K_1](r_1 + r_2) \\ \implies \ddot{\sigma}(t, x, \sigma, \dot{\sigma}) \in [c_1 - K_1(r_1 + r_2), C_1 - k_1(r_1 + r_2)]. \end{aligned} \quad (46)$$

Doing the same computation in the other domains Σ_i yields the bounds,

$$\begin{aligned} m_1^1 &= c_1 - K_1(r_1 + r_2), \quad M_1^1 = C_1 - k_1(r_1 + r_2), \\ m_2^1 &= c_2 - K_2(r_1 - r_2), \quad M_2^1 = C_2 - k_2(r_1 - r_2), \\ m_3^1 &= c_3 + k_3(r_1 + r_2), \quad M_3^1 = C_3 + K_3(r_1 - r_2), \\ m_4^1 &= c_4 + k_4(r_1 - r_2), \quad M_4^1 = C_4 + K_4(r_1 - r_2). \end{aligned} \quad (47)$$

By injecting these bounds into Conditions (13), (14), (15), one gets Conditions (43), (44), (45). It follows that if the conditions of Corollary 1.1 are satisfied, then the conditions of Theorem 1 are also satisfied. ■

Corollary 1.1 states directly conditions on (r_1, r_2) that ensure finite-time convergence, provided that bounds k_i, K_i, c_i, C_i are known, whereas Theorem 1 states conditions only on the bounds m_i, M_i but not on the tunable parameters. This is due to the fact that the bounds (47) considered in Corollary 1.1 are explicit functions of r_1, r_2 and injecting them into the conditions of Theorem 1 makes them into conditions on r_1, r_2 .

Finally, Corollary 1.2 proposes more conservative conditions than Corollary 1.1 but requires only bounds on h and g over X instead of the four sub-spaces X_i . Corollary 1.2 provides the well-known convergence conditions of the twisting algorithm (Levant, 1993), and is stated as in Shtessel et al. (2014). The proof is nevertheless provided to make the connection with Theorem 1.

Corollary 1.2 (Shtessel et al. (2014, pp. 148)). Consider the system (4) with the twisting controller (5). Let C be an upper bound on $|h|$ over the state space,

$$|h(t, x)| \leq C, \forall x \in X, \forall t \geq 0, \quad (48)$$

and k, K be bounds on g ,

$$g(t, x) \in [k, K], \forall x \in X, \forall t \geq 0. \quad (49)$$

If (r_1, r_2) satisfies

$$\begin{aligned} k > 0, \\ 0 < r_2 < r_1, \end{aligned} \quad (50)$$

$$C < k(r_1 - r_2), \quad (51)$$

and

$$(r_1 - r_2)K + C < (r_1 + r_2)k - C, \quad (52)$$

then σ and $\dot{\sigma}$ converge to zero in finite time. ■

Proof. In a similar way as in the proof of Corollary 1.1, and due to Condition (50), one gets the bounds on $\ddot{\sigma}$,

$$\begin{aligned} m_1^2 &= -C - K(r_1 + r_2), \quad M_1^2 = C - k(r_1 + r_2), \\ m_2^2 &= -C - K(r_1 - r_2), \quad M_2^2 = C - k(r_1 - r_2), \\ m_3^2 &= -C + k(r_1 + r_2), \quad M_3^2 = C + K(r_1 + r_2), \\ m_4^2 &= -C + k(r_1 - r_2), \quad M_4^2 = C + K(r_1 - r_2). \end{aligned} \quad (53)$$

With these bounds, Condition (51) implies Conditions (13), (14) of Theorem 1 and Condition (52) implies Condition (15) ■

3.3. Discussion

The convergence conditions of Theorem 1 and Corollaries 1.1 and 1.2 reveal three levels of conservatism. Indeed, it can be noticed that if the conditions of Corollary 1.2 are satisfied, then the conditions of Corollary 1.1 are satisfied by considering

$$\begin{aligned} C_i &= -c_i = C, \\ k_i &= k, \\ K_i &= K. \end{aligned} \quad (54)$$

Furthermore, if the conditions of Corollary 1.1 are satisfied, then the conditions of Theorem 1 are satisfied as shown in the proof of Corollary 1.1. As a consequence, there is an implication relationship between the conditions of Theorem 1 and Corollaries 1.1 and 1.2.

The conservatism can be further explained by the quality of the bounds on $\ddot{\sigma}$ that can be used by the different convergence conditions. The conditions of Theorem 1 allow to consider tighter bounds on $\ddot{\sigma}$ than the conditions of Corollary 1.1, which themselves can be used with tighter bounds than the conditions of Corollary 1.2 due to the expression of these bounds. The tightest enclosure $[m_i^{1*}, M_i^{1*}]$ that can be derived from bounds (47) is obtained with

$$\begin{aligned} c_i^* &= \inf_{\substack{t \geq 0 \\ x \in X_i(t)}} h(t, x), \quad C_i^* = \sup_{\substack{t \geq 0 \\ x \in X_i(t)}} h(t, x), \\ k_i^* &= \inf_{\substack{t \geq 0 \\ x \in X_i(t)}} g(t, x), \quad K_i^* = \sup_{\substack{t \geq 0 \\ x \in X_i(t)}} g(t, x), \end{aligned} \quad (55)$$

and the tightest enclosure $[m_i^{2*}, M_i^{2*}]$ that can be derived from bounds (53) is obtained with

$$\begin{aligned} C^* &= \sup_{\substack{t \geq 0 \\ x \in X}} |h(t, x)|, \\ k^* &= \inf_{\substack{t \geq 0 \\ x \in X}} g(t, x), \quad K^* = \sup_{\substack{t \geq 0 \\ x \in X}} g(t, x). \end{aligned} \quad (56)$$

These bounds are such that,

$$[m_i^*, M_i^*] \subseteq [m_i^{2*}, M_i^{2*}] \subseteq [m_i^{3*}, M_i^{3*}], \quad (57)$$

and equal only in particular cases. As a consequence, using the conditions of Theorem 1 with m_i^{2*}, M_i^{2*} is more conservative than using them with m_i^*, M_i^* , which is more conservative than using m_i^{3*}, M_i^{3*} .

Remark 2. Being less conservative means that the new conditions describe a larger set of convergent tuning. The most typical objective being to use small gains, the new conditions will lead to smaller gains using such a performance objective. This can be in contradiction with other objectives like the converging time.

The twisting controller is appropriate if $\ddot{\sigma}$ has the affine expression (7) and g is positive. In this case, choosing r_1 and r_2 sufficiently large ensures the convergence conditions. However, Theorem 1 can be applied in the general case where $\ddot{\sigma}$ in non-linear in u , and the twisting controller may not always be a relevant control structure to ensure the convergent conditions. This is emphasized by the second example in Section 4.

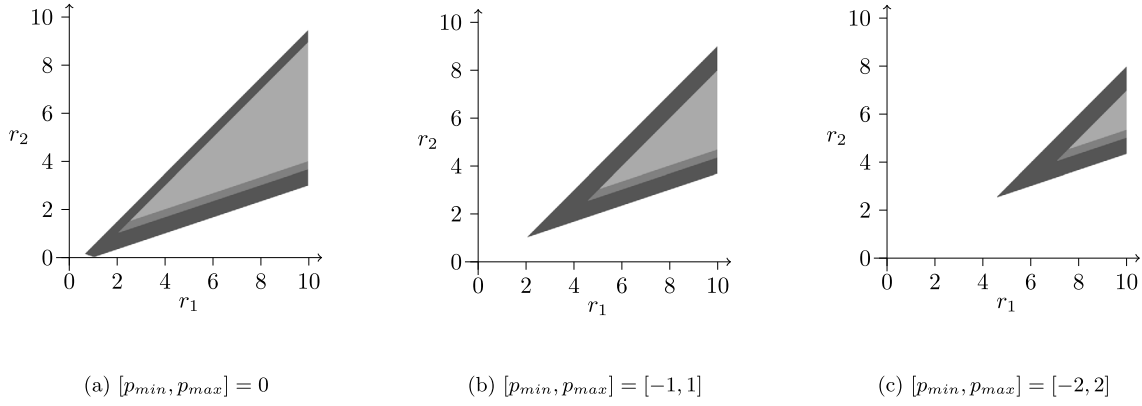


Fig. 2. Sets of (r_1, r_2) values that ensure establishment of 2-SM resulting from the convergence conditions. Dark gray: [Theorem 1](#), gray: [Corollary 1.1](#), light gray: [Corollary 1.2](#).

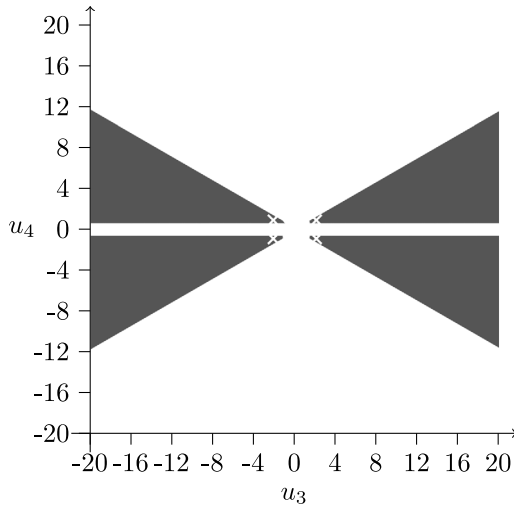


Fig. 3. Sets of (u_3, u_4) values that ensure establishment of 2-SM resulting from the conditions of [Theorem 1](#). The white crosses represent the values used for simulation.

4. Academic examples

This section proposes to study two examples. The first one illustrates the different levels of conservatism of the three corollaries. The second example shows that [Theorem 1](#) can be employed in the case where $\ddot{\sigma}$ is non-affine in u . The software Mathematica was used to generate [Figs. 2 and 3](#).

4.1. Example 1: Conservatism illustration

Consider the system

$$\begin{aligned} \dot{x}_1 &= x_2, \\ \dot{x}_2 &= x_1 + (1 + |x_1|)u + p(t), \end{aligned} \quad (58)$$

with p an unknown perturbation bounded in $[p_{min}, p_{max}]$. Notice that this system has a form similar to (4) with $h(t, x) = x_1 + p(t)$ and $g(t, x) = 1 + |x_1|$. The sliding variable is defined as $\sigma = x_1$. Supposing that the system is controlled by a twisting controller, the second time derivative of the sliding variable reads as

$$\ddot{\sigma} = x_1 + (1 + |x_1|)(-r_1 \text{sign}(x_1) - r_2 \text{sign}(x_2)) + p(t). \quad (59)$$

It follows that h and g are expressed as,

$$h(x, t) = x_1 + p(t), \quad g(x) = 1 + |x_1|. \quad (60)$$

For this example, the expressions of m_i and M_i can be determined by studying the sign of

$$\frac{\partial \ddot{\sigma}}{\partial x_1} = 1 + \text{sign}(x_1)(-r_1 \text{sign}(x_1) - r_2 \text{sign}(x_2)), \quad (61)$$

that depends only on r_1 and r_2 in the four sub-spaces X_i . In the following, state $r_1 > r_2 > 0$ and limit the study to the bounded subset of the state space $X = [-1, 1] \times [-1, 1]$. Computations yield the following bounds.

- In $X_1 =]0, 1[\times]0, 1[$, one has $C_1^* = 1, k_1^* = 1$ and

$$M_1^* = \begin{cases} 1 - 2(r_1 + r_2) + p_{max} & \text{if } r_1 + r_2 < 1, \\ -(r_1 + r_2) + p_{max} & \text{otherwise.} \end{cases} \quad (62)$$

- In $X_2 =]0, 1[\times]-1, 0[$, one has $c_2^* = 0, C_2^* = 1, k_2^* = 1, K_2^* = 2$ and

$$M_2^* = \begin{cases} -r_1 + r_2 + p_{min} & \text{if } r_1 - r_2 < 1, \\ 1 + 2(-r_1 + r_2) + p_{min} & \text{otherwise,} \\ 1 + 2(-r_1 + r_2) + p_{max} & \text{if } r_1 - r_2 < 1, \\ -r_1 + r_2 + p_{max} & \text{otherwise.} \end{cases} \quad (63)$$

- In $X_3 =]-1, 0[\times]1, 0[$, one has $c_3^* = -1, k_3^* = 1$ and

$$M_3^* = \begin{cases} -1 + 2(r_1 + r_2) + p_{min} & \text{if } r_1 + r_2 < 1, \\ r_1 + r_2 + p_{min} & \text{otherwise,} \end{cases} \quad (64)$$

- In $X_4 =]-1, 0[\times]0, 1[$, one has $c_4^* = -1, C_4^* = 0, k_4^* = 1, K_4^* = 2$ and

$$M_4^* = \begin{cases} -1 + 2(r_1 - r_2) + p_{min} & \text{if } r_1 - r_2 < 1, \\ r_1 - r_2 + p_{min} & \text{otherwise,} \\ r_1 - r_2 + p_{max} & \text{if } r_1 - r_2 < 1, \\ -1 + 2(r_1 - r_2) + p_{max} & \text{otherwise.} \end{cases} \quad (65)$$

Conditions of [Theorem 1](#) and [Corollaries 1.1 and 1.2](#), are used to characterize sets of pairs (r_1, r_2) for three different bounds $[p_{min}, p_{max}]$. In the first case, suppose that there is no perturbation, $p_{min} = p_{max} = 0$. In the two other cases, we use $p_{max} = -p_{min} = 1$ and $p_{max} = -p_{min} = 2$. The set of pairs (r_1, r_2) defined by the constraints of [Theorem 1](#) with the bounds m_i^*, M_i^* is represented by the dark gray areas in [Fig. 2](#). By [Theorem 1](#), any value (r_1, r_2) in these dark gray sets guarantees the finite time establishment of a 2-SM.

The values k_i are all positive and satisfy Condition (42) of [Corollary 1.1](#). Conditions (42) to (45) of [Corollary 1.1](#) with $c_i^*, C_i^*, k_i^*, K_i^*$ define the sets represented in gray in [Fig. 2](#).

From the bounds on g and h over the four sub-spaces X_i , we derive $C^* = 1$ and $[k^*, K^*] = [1, 2]$. The set defined by Conditions

(50) and (51) of Corollary 1.2 using C^* , k^* , K^* provide the light gray sets in Fig. 2.

It can be seen in Fig. 2 that the light gray set defined by the conditions of Corollary 1.2 is contained in the gray set, defined by the conditions of Corollary 1.1, which is itself a subset of the dark gray set defined by the conditions of Theorem 1. This illustrates the different levels of conservatism of the three Corollaries yields by the inclusion (57).

4.2. Example 2 : Non-affine system

Consider the dynamical system

$$\begin{aligned} \dot{x}_1 &= x_2, \\ \dot{x}_2 &= -2 + x_2 + u^2, \end{aligned} \quad (66)$$

for $x_1, x_2 \in [-1, 1]$. The sliding variable is chosen as $\sigma = x_1$. It follows that the second time derivative of σ reads as

$$\ddot{\sigma} = -2 + x_2 + u^2. \quad (67)$$

However, Theorem 1 does not require $\ddot{\sigma}$ to be affine in u and can be employed to find a control u that ensures finite-time convergence. To do so, compute m_i and M_i as functions of u .

- In $X_1 =]0, 1[\times]0, 1[$, one has $M_1^* = -1 + u^2$.
- In $X_2 =]0, 1[\times]-1, 0[$, one has $m_2^* = -3 + u^2$ and $M_2^* = -2 + u^2$.
- In $X_3 =]-1, 0[\times]-1, 0[$, one has $m_3^* = -3 + 4u^2$.
- In $X_4 =]-1, 0[\times]0, 1[$, one has $m_4^* = -2 + 4u^2$, and $M_4^* = -1 + 4u^2$.

Condition (13) imposes $-1 + u^2 < 0$ in X_1 whereas Condition (14) imposes $-3 + u^2 > 0$ in X_3 . With the twisting controller (5), these conditions become

$$\begin{aligned} -1 + (-r_1 - r_2)^2 &< 0, \\ -3 + (r_1 + r_2)^2 &> 0. \end{aligned} \quad (68)$$

As a consequence, there exists no (r_1, r_2) such that the twisting controller enforces these two conditions.

Let us consider a more general controller structure than the twisting controller, given by,

$$u = u_i \text{ if } (\sigma, \dot{\sigma}) \in \Sigma_i, \quad (69)$$

with $u_i \in \mathbb{R}$. With controller (69), Condition (13) becomes,

$$-1 < u_1 < 1, \quad -\sqrt{2} < u_2 < \sqrt{2}, \quad (70)$$

and Condition (14) becomes,

$$\begin{aligned} u_3 \in]-\infty, -\sqrt{3}/2[\cup]\sqrt{3}/2, \infty[, \\ u_4 \in]-\infty, -1/\sqrt{2}[\cup]1/\sqrt{2}, \infty[. \end{aligned} \quad (71)$$

Choosing arbitrarily $u_1 = u_2 = 0$, Condition (15) rewrites,

$$(-1)(-3 + 4u_3^2) < (-3)(-1 + 4u_4^2) \quad (72)$$

The set of values for (u_3, u_4) satisfying the convergence conditions are represented by the dark gray set in Fig. 3. Fig. 4 displays the simulation of the system with the initial condition $(\sigma_0, \dot{\sigma}_0) = (0, 0.8)$ and the parameters $(u_3, u_4) = (2.1, 0.9)$. As one can remark, the system converges by a twisting convergence even if $\dot{\sigma}$ moves away from the origin in the half space $\sigma > 0$.

5. Conclusion

In this paper, new convergence conditions that are not limited to systems that are affine in the control nor to the twisting controller structure are proposed in order to guarantee the finite time convergence. The approach relies on considering a piecewise set vector field over several domain of the phase plan,

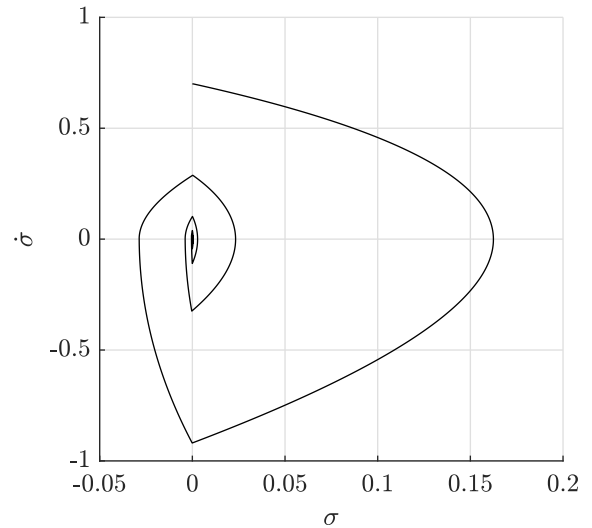


Fig. 4. Phase diagram of Example 2 simulated with $(u_3, u_4) = (2.1, 0.9)$ or equivalently $(2.1, -0.9)$, $(-2.1, 0.9)$ or $(-2.1, -0.9)$.

that enables to ignore the underlying system and interconnected controller. It was shown over two academic examples that the new conditions

- (1) are less conservative than state-of-the-art conditions based on majorant curve for affine systems,
- (2) can enforce a twisting convergence for non-affine systems.

In particular, the second example illustrated that the twisting controller might not ensure twisting-like convergence of non-affine systems. A more flexible control structure was proposed that enabled to meet the convergence conditions. Although more flexible, this structure might not work for any non-affine plants. Future work includes finding control strategies for large classes of non-affine plants.

The examples featured in Section 4 could be solved analytically, but that might not be possible for more complex real case problems. Indeed, it is not always possible to derive explicit expressions of bounds on $\ddot{\sigma}$ in the non-affine case. However, $\ddot{\sigma}$ has an explicit expression depending on r , which makes it possible employ a global non-convex numerical solver to compute these bounds (Sahinidis, 1996). A numerical approach would spare the search of analytic solutions, and enable to consider more complex and flexible control structure to ensure the convergence of non-affine plants. Future work includes the formulation of the problems as programs that can be solved with numerical solvers.

Another direction for future research would be to extend the generalized approach based on piece-wise differential inclusion proposed in this paper to other existing 2-SM algorithms, such as the super-twisting.

Acknowledgments

The authors would like to thank the reviewers for their helpful comments.

References

- Boiko, Igor (2005). Analysis of sliding modes in the frequency domain. *International Journal of Control*, 78(13), 969–981.
- Davila, Jorge, Fridman, Leonid, & Levant, Arie (2005). Second-order sliding-mode observer for mechanical systems. *IEEE Transactions on Automatic Control*, 50(11), 1785–1789.
- Edwards, Christopher, & Spurgeon, Sarah (1998). *Sliding Mode Control: Theory and Applications*. Boca Raton, USA: Taylor & Francis.

- Ferrara, Antonella, Incremona, Gian Paolo, & Cucuzzella, Michele (2019). *Advanced and Optimization Based Sliding Mode Control: Theory and Applications*. SIAM.
- Filippov, Aleksey F. (2010). *Differential Equations with Discontinuous Righthand Sides: Control Systems*. The Netherlands: Kluwer, Dordrecht.
- Fridman, Leonid M. (2003). Chattering analysis in sliding mode systems with inertial sensors. *International Journal of Control*, 76(9–10), 906–912.
- Fridman, Leonid M., Barbot, Jean-Pierre, & Plestan, Franck (2016). *Recent Trends in Sliding Mode Control*. London, UK: The Institution of Engineering and Technology.
- Incremona, Gian Paolo, Cucuzzella, Michele, & Ferrara, Antonella (2017). Second order sliding mode control for nonlinear affine systems with quantized uncertainty. *Automatica*, 86, 46–52.
- Levant, Arie (1993). Sliding order and sliding accuracy in sliding mode control. *International Journal of Control*, 58(6), 1247–1263.
- Levant, Arie (1998). Robust exact differentiation via sliding mode technique. *Automatica*, 34(3), 379–384.
- Levant, Arie (2007). Principles of 2-sliding mode design. *Automatica*, 43(4), 576–586.
- Levant, Arie (2010). Chattering analysis. *IEEE Transactions on Automatic Control*, 55(6), 1380–1389.
- Moreno, Jaime A., & Osorio, Marisol (2008). A Lyapunov approach to second-order sliding mode controllers and observers. In *IEEE Conference on Decision and Control* (pp. 2856–2861).
- Moreno, Jaime A., & Osorio, Marisol (2012). Strict Lyapunov functions for the super-twisting algorithm. *IEEE Transactions on Automatic Control*, 57(4), 1035–1040.
- Polyakov, Andrei, & Poznyak, Alex (2009). Lyapunov function design for finite-time convergence analysis: “twisting” controller for second-order sliding mode realization. *Automatica*, 45(2), 444–448.
- Sahinidis, Nikolaos V. (1996). BARON: A general purpose global optimization software package. *Journal of Global Optimization*, 8(2), 201–205.
- Shtessel, Yuri B., Edwards, Christopher, Fridman, Leonid M., & Levant, Arie (2014). *Sliding mode control and observation*. New York, USA: Springer.
- Shtessel, Yuri B., Moreno, Jaime A., & Fridman, Leonid M. (2017). Twisting sliding mode control with adaptation: Lyapunov design, methodology and application. *Automatica*, 75, 229–235.
- Shtessel, Yuri B., Moreno, Jaime A., Plestan, Franck, Fridman, Leonid M., & Poznyak, Alexander S. (2010). Super-twisting adaptive sliding mode control: A Lyapunov design. In *IEEE Conference on Decision and Control* (pp. 5109–5113).
- Shtessel, Yuri B., Taleb, Mohammed, & Plestan, Franck (2012). A novel adaptive-gain supertwisting sliding mode controller: Methodology and application. *Automatica*, 48(5), 759–769.

Utkin, Vadim I. (2013). *Sliding Modes in Control and Optimization*. Springer Science & Business Media.

Utkin, Vadim I., Guldner, Jürgen, & Jingxin, Shi (2009). *Sliding Mode Control in Electro-Mechanical Systems* (Second edition). CRC Press.



Dominique Monnet received both his engineer diploma, in 2014, and his Ph.D. in automatic control, in 2018, from ENSTA Bretagne, France. He was a post-doctoral fellow at the University of British Columbia, Canada, in 2019 and Ecole Centrale de Nantes, France, in 2020. He joined Polytechnique Montreal, Canada, in 2021 as a postdoctoral fellow. His research interests include the development of non-linear optimization tools to solve design problems arising in different fields of automatic control, such as H infinity synthesis or sliding mode control.



Alexandre Goldsztejn received his engineer degree from the Institut Supérieur d'Electronique et du Numérique, Lille, France, in 2001, and his Ph.D. in Computer Science from the University of Nice-Sophia Antipolis in 2005. He has spent one year as a post-doctoral fellow in the University of Central Arkansas and the University of California Irvine. His research interests include interval analysis and its application to constraint satisfaction, nonlinear global optimization, robotics and control.



Franck Plestan received the Ph.D. in Automatic Control from the Ecole Centrale de Nantes, France, in 1995. From September 1996 to August 2000, he was with Louis Pasteur University, Strasbourg, France. In September 2000, he joined the Ecole Centrale de Nantes, Nantes, France where he is currently Professor. His research interests include robust control (adaptive/higher order sliding mode, time-delay systems) and nonlinear observer design. He is also working in several application domains as pneumatic actuators, automotive, flying systems, renewable energy systems.